Received Date : 14-Apr-2016
Revised Date : 14-Jul-2016
Accepted Date : 23-Sep-2016
Article type : Research Article

Synthesis and preliminary evaluation of a ^{18}F-labeled ethisterone derivative [^{18}F]EAEF for progesterone receptor targeting

Xiaowei Wu[a], Linyi You[a], Deliang Zhang[a], Mengna Gao[a], Zijing Li[a], Duo Xu[a], Pu Zhang[a], Lumei Huang[a], Rongqiang Zhuang[a], Hua Wu[b], Xianzhong Zhang[a,*]

a. Center for Molecular Imaging and Translational Medicine, State Key Laboratory of Molecular Vaccinology and Molecular Diagnostics, School of Public Health, Xiamen University, Xiamen, Fujian 361102, China.

b. The First Affiliated Hospital of Xiamen University, Zhenhai Road, Xiamen 361003, China.

***For correspondence contact:**

Xianzhong Zhang, PhD, Professor

Center for Molecular Imaging and Translational Medicine, School of Public Health, Xiamen University

Xiang'an South Rd., Xiang'an district, Xiamen 361102, China.

E-mail: zhangxzh@xmu.edu.cn; Phone: +86-592-2880645, Fax: +86-592-2880645

First author

Xiaowei Wu, graduate student

Center for Molecular Imaging and Translational Medicine, School of Public Health, Xiamen University

Xiang'an South Rd., Xiang'an district, Xiamen 361102, China.
E-mail: 976074235@qq.com; Phone: +86-592-2880641

Contract/grant sponsor: This study was financially supported by the National Key Basic Research Program of China (2014CB744503) and National Natural Science Foundation of China (81471707, 21271030).

Abstract

To develop a novel progesterone receptor (PR) targeting probe for positron emission tomography (PET) imaging, ethisterone derivative [^{18}F]EAEF was designed and prepared in high decay-corrected radiochemical yield (30 ~ 35%) with good radiochemical purity (> 98%). [^{18}F]EAEF is a lipophilic tracer (log*P* = 0.53 ± 0.06) with very good stability in saline and serum. In the biodistribution study, high radioactivity accumulation of [^{18}F]EAEF were found in uterus (5.73 ± 1.83 % ID/g) and ovary (4.05 ±0.73 % ID/g) at 2 h post-injection (p.i.), which have high PR expression after treated with estradiol, while the muscle background has very low uptake (0.50 ± 0.17 % ID/g). For PET imaging, [^{18}F]EAEF showed high uptake in PR positive MCF-7 tumor (3.15 ± 0.07 % ID/g at 2 h p.i.) with good tumor-to-muscle ratio (2.90), and obvious lower tumor uptakes were observed in MCF-7 with EAEF blocking (1.84 ± 0.05 % ID/g at 2 h p.i.) or in PR negative MDA-MB-231 tumor (1.80 ± 0.03 % ID/g at 2 h p.i.). Based on the good stability and specificity of [^{18}F]EAEF, it may be a good candidate for imaging PR and worth further investigation.

Keywords: Fluorine-18; Positron emission tomography; Breast cancer; Progesterone receptor; Ethisterone

Running title: [^{18}F]EAEF for PR imaging with PET

1. Introduction

Early diagnosis of breast cancer, which seriously endangers the women all over the world, could effectively promote the curative effect and reduce the mortality rate(1, 2). However, with high heterogeneity and various kinds of tissue subtypes, the breast cancer has different clinical manifestations, as well as individual therapeutic responses and prognosis(3-5). Screening mammography used to be a major imaging method for the early detection and diagnosis of breast cancer in the past, its false positive occurred frequently in the diagnosis(6, 7). In the meanwhile, early molecular typing of tumor through comprehensive molecular imaging techniques will provide more information for the classification of tumors, speeding up tumor classification based on morphological steering on molecular characteristics as a new and more reliable basis of tumor classification(8). Compared with mammography, diagnose breast cancer by PET has been developed to image breast-cancer-relative receptors using targeting molecules labeled with position-emitting radionuclides(9). Furthermore, nuclear medical imaging is able to provide high sensitivity, non-invasive detection as well as providing information about the biological process of tumor superior to the mammography(10, 11).

Progesterone plays an important role in the female reproductive system through the combination of PR(12), which mediating and regulating the function of ovary, uterus and mammary gland(13, 14). Because PR expression is depending on the estrogen receptor (ER), so it is rare to have the subtype ER+/PR- of breast cancer(15). Many studies showed that in

ER+ patients, PR expressed or not will not have a significant influence on the advantages toward the tamoxifen treatment. While in ER- patients, the benefit got from tamoxifen will depend on the status of PR(16-18). So, monitoring the PR expression is crucial for not only early diagnosis of breast cancer but also curing ER-/PR+ type of breast cancer. Herein, we designed and synthesized a small molecular probe derived from ethisterone to target the PR in breast cancer for the detection of progesterone receptor overexpression with PET imaging.

Modified steroid structures were usually used as probes to target PR, such as progesterone, testosterone and 19-nortestosterone, and different modifications of these structures will affect the binding affinity(11). Until now, tens of steroids, such as 21-[^{18}F]Fluoro-16α-ethyl-19-norprogesterone ([^{18}F]FENP), 21-[^{18}F]Fluoro-16α-methyl-19-norprogesterone ([^{18}F]FMNP), 6α-[^{18}F]Fluoroprogesterone and 4-[^{18}F] Fluoropropyl-tanaproget ([^{18}F]FPTP) (**Figure 1**), have been reported as PR targeted imaging agents and evaluated *in vivo* and *in vitro*. However, only a few of these radiotracers have been tested in pre-clinical and clinical trials.

As a natural progesterone derivative, ethisterone binds to PR with high affinity, and its alkynyl group can be easily modified compared with other steroids. Herein in this study, an ethisterone based novel probe was designed and synthesized for PR targeted imaging. Since ^{18}F has an ideal half-time (110 min), high spatial resolution, low positron energy (0.635 MeV), we tried to develop a ^{18}F-labeled steroid for PET imaging of PR.

Materials and methods

Chemicals and equipments

All reagents and solvents were purchased from commercial suppliers. HPLC was carried out with a NUCLEOSIL C18 reversed-phase column (100 × 10, 5μm particle size), working at a flow rate of 1.0 mL/min. The radioactivity counts were measured with γ-counter (WIZARD 2480, Perkin-Elmer, USA) and CRC-25R Dose Calibrators (CAPINTEC.INC, USA). Imaging study was performed by a micro PET/CT (SIEMENS). ^{1}H NMR spectra and ^{13}C NMR spectra were measured on an AVANCE III 600 MHz spectrometer. Chemical shifts were reported in δ (ppm) values. Mass spectra (MS) were recorded using a Q Exactive LC-MS/MS instrument.

*Preparation of compound **2***

Triethylene glycol (3.00 g, 0.02 mol) was dissolved in 20.0 mL of anhydrous CH_2Cl_2 and triethylamine (10.00 g, 0.10 mol), 4-toluene sulfochloride (19.00 g, 0.10 mol) were added. The solution was stirred overnight. After reaction, the solvent was evaporated in vacuo to give the residue. Ethyl acetate (100 mL) was added and washed with brine (100 mL), and the organic layer was dried with Na_2SO_4. The solvent was evaporated in vacuo to give the residue which was purified by column chromatography (silica gel, petroleum ether/ ethyl acetate 2:1) to give the white solid of compound **2** (28.10 g, 61.40 mmol, 88.4%). ^{1}H NMR (600 MHz, $CDCl_3$) δ 7.79 (d, 4H, *J* = 12 Hz), 7.34 (d, 4H, *J* = 12 Hz), 4.14 (t, 4H, *J* = 6 Hz), 3.66 (t, 4H, *J* = 3 Hz), 3.52 (s, 4H), 2.45 (s, 6H); ^{13}C NMR (150 MHz, $CDCl_3$) δ144.9, 132.8,

129.9, 128.1, 70.7, 69.2, 68.7, 21.7. MS: m/z $[M+Na]^+$ = 481.1.

*Preparation of compound **3***

Compound **2** (1.00 g, 2.20 mmol) was dissolved in 20 mL of anhydrous CH_3CN and NaN_3 (71.00 mg, 1.10 mmol) was added, the mixture were heated to reflux for 8 h at 85 ℃. After reaction, the solvent was evaporated in vacuo to give the residue. Ethyl acetate (80 mL) was added and washed with brine (80 mL), and the organic layer was dried with Na_2SO_4. The solvent was evaporated in vacuo and purified by column chromatography (silica gel, petroleum ether/ ethyl acetate 8:1) to give the white oil of compound **3** (0.50 g, 61.40 mmol, 69.90%).

^{1}H NMR (600 MHz, $CDCl_3$) δ 7.79 (m, 2H), 7.35 (m, 2H), 4.16 (m, 2H), 3.70 (m, 2H), 3.64(m, 2H), 3.60 (s, 4H), 3.36 (dt, 2H, J_1 = 18 Hz, J_2 = 6 Hz), 2.44 (s, 3H); ^{13}C NMR (150 MHz, $CDCl_3$) δ 145, 133.2, 130.5, 128.1, 70.8, 70.7, 70.1, 69.3, 68.8, 50.7, 21.7. MS: m/z $[M+Na]^+$ = 352.1.

*Preparation of compound **4** (precursor)*

Compound **3** (80.00 mg, 0.20 mmol) was dissolved in tetrahydrofuran and CuI (3.00 mg, 0.02 mmol), N,N-Diisopropylethylamine (37.16 mg, 0.49 mmol), ethisterone (45.00 mg, 0.14 mmol) were added, the mixture were heated to reflux for 6 h at 85 ℃. After reaction, the solvent was evaporated in vacuo to give the residue. Ethyl acetate (30 mL) was added and washed with brine (50 mL), and the organic layer was dried with Na_2SO_4. The solvent was evaporated in vacuo and purified by column chromatography (silica gel, petroleum ether/

ethyl acetate 2:1) to give the white oil of compound **4** (60.10 mg, 0.12 mmol, 65.00%).

^{1}H NMR (600 MHz, $CDCl_3$) δ 7.56 (s, H), 5.70 (s, H), 4.59 (t, H, J = 12 Hz), 4.52 (m, 3H), 3.88(m, 2H), 3.66 (dd, 2H, J_1 = 3.6 Hz, J_2 = 6 Hz), 3.56 (m, 4H), 0.48-2.00 (m, 26H); ^{13}C NMR (150 MHz, $CDCl_3$) δ 199.6, 171.4, 153.5, 145, 132.9, 129.9, 128, 123.8, 122.4, 82, 70.8, 70.5, 69.7, 69.2, 68.8, 53.3, 50.3, 48.9, 46.9, 38.6, 37.8, 36.4, 35.6, 33.9, 32.9, 32.7, 31.6, 21.7, 21.1, 20.6, 17.4, 14.3.

Preparation of EAEF

Compound **4** (30.00 mg, 0.05 mmol) was dissolved in 2 mL of anhydrous CH_3CN and KF (13.60 mg, 0.23 mmol), Kryptofix222 (35.2 mg, 0.09 mmol) were added, the mixture were heated to reflux for 10 h at 90 ℃. After reaction, the solvent was evaporated in vacuo to give the residue. Ethyl acetate (30 mL) was added and washed with brine (50 mL), and the organic layer was dried with Na_2SO_4. The solvent was evaporated in vacuo and purified by column chromatography (silica gel, petroleum ether/ ethyl acetate 1:1) to give the white oil of EAEF (13.72 mg, 0.03 mmol, 62.00%).

^{1}H NMR (600 MHz, $CDCl_3$) δ 7.78 (d, 2H), 7.57 (s, H), 7.34 (d, 2H), 5.69 (s, H), 4.52(s, 2H), 4.15 (t, 3H), 3.85 (d, 2H), 3.63 (m, 2H), 3.56 (s, 4H), 2.45 (s, 3H), 0.47-2.37 (m, 26H); MS: m/z $[M+H]^+$ = 490.1.

Radiolabeling

In **Scheme 1**, compound **3** was coupled with ethisterone to obtain compound **4**. Then after it was radiofluorinated by replacing of tosylate group to get the final probe [^{18}F]EAEF(19).

Briefly, after eluted the [^{18}F]fluoride from the QMA cartridge (Waters light Sep-Pak, which was pretreated with 20 mL of K_2CO_3 (1 mol/L) and 20 mL H_2O) with 1 mL eluate (CH_3CN/H_2O = 900 μL /100 μL containing 13 mg Kryptofix222 and 1.1 mg K_2CO_3) into the reaction vial. Then the reactant was dried with anhydrous CH_3CN three times under 120 ºC to remove water. Afterward, 2 mg compound **4** was added, and reacted in anhydrous CH_3CN at 90 ºC for 20 min.

Octanol/water partition coefficient

Determination of octanol/water partition coefficient (*P*) was performed by the following method: About 0.185 MBq [^{18}F]EAEF was added to a solution containing 200 μL of 1-octanol and 200 μL of water. After vortexed at room temperature for 10 min. Aliquots (50 μL) of both organic and inorganic layers were removed from the mixtures, and the radioactivity were measured in a Wizard 2480 automatic γ-counter. The experiment was repeated three times.

Stability study

The stability of [^{18}F]EAEF was tested in saline and mouse serum, respectively. About 3.7 MBq [^{18}F]EAEF was added to 900 μL of saline (or mouse serum) and incubated at 37 ºC for 30 min, 60 min, and 120 min. Then the samples were analyzed by HPLC after passing through a C-18 column with 0.4 mL CH_3CN and 0.6 mL water per minute.

Biodistribution study

The biodistribution of [^{18}F]EAEF was evaluated in normal ICR mouse (18-20 g, female). The experimental procedures and the animal use and care protocols were approved by the Xiamen University's animal care and use committee. The progesterone receptor levels of immature mice were induced by subcutaneous injection of 3 μg estradiol in 100 μL 10% ethanol/water 2 times (one time/day). The study was carried out 24 h after the last injection. About 0.74 MBq [^{18}F]EAEF were intravenous (i.v.) injected in mice via tail vein. At 1 and 2 h p.i., the mice were sacrificed by decapitation, then the blood and interested organs were removed, weighed and counted in a γ-counter. To testify the high-affinity and specific uptake of [^{18}F]EAEF, biodistribution at 2 h p.i. was also performed in mice without estradiol treated. The percentage injected dose per gram of tissue (% ID/g) was calculated by compared with standards representing the injected dose per animal. The final result were expressed as mean ± SD (n = 4, **Table 1**).

Imaging study

To evaluate the feasibility of *in vivo* PET imaging with [^{18}F]EAEF for PR positive tumor detection. Xenografted MCF-7 (PR+) and MDA-MB-231 (PR-) tumor models were established in female BALB/C nude mice (6-week-old). The mice were obtained from the Laboratory Animal Center of Xiamen University and all animal experiments were carried out in accordance with the guidelines and approved protocols established by the Xiamen University's animal care and use committee. Tumor models were generated by injecting 2-3 million MCF-7 cells and MDA-MB-231 cells subcutaneously in nude mice on the right

shoulder and the consequent tumors were allowed to grow for 14-16 days. Imaging data were acquired using Inveon microPET/CT (SIEMENS) at 15 min, 1 h, 2 h and 4 h after injection of 3.7 MBq of [^{18}F]EAEF via tail vein under isoflurane anesthesia on a temperature-controlled bed.

In order to test the specifivity of [^{18}F]EAEF, PET imaging studies with 200 μg precursor or EAEF blocking, or pre-treated with 200 μg ethisterone were performed in PR positive MCF-7 tumor bearing mice.

All images were performed in the same manners and reconstructed, processed and analyzed with Inveon Research Workplace program (SIEMENS).

Results

Chemistry

Scheme **1** shows the synthetic route of compound **4**. First of all, 2-(2-(2-azidoethoxy)eth-oxy)ethyl-4-*p*-toluenesulfonate was prepared from triethylene glycol (TEG) according to the described work by Achim T. Reibel et al. (19). Then, compound **4** was obtained by the reaction of 2-(2-(2-azidoet-hoxy)ethoxy) ethyl-4-*p*-toluenesulfonate with ethisterone in the presence of CuI and N,N-diisopropylethylamine (DIPEA). All of the compounds have high chemical yields and were characterized by MS, ^{1}H NMR, or ^{13}C NMR.

Radiochemistry

Preparation of the [^{18}F]EAEF was isolated to provide a decay-corrected radiochemical yield (RCY) of 30 - 35% with a specific activity of (96.04 ± 15.50) GBq/μmol (n=3) with

simple and time saving one-step radiolabeling process. High radiochemical purity (RCP, > 98%) was also obtained after reversed-phase high performance liquid chromatography (HPLC) purification (NUCLEOSIL 100-10 C18 column; isocratic method of H_2O/CH_3CN = 60/40 at flow rate of 1 mL/min). In order to characterize the radiolabeled probe [^{18}F]EAEF, the non-radioactivity EAEF was also synthesized and characterized as reference. The chemical identities of [^{18}F]EAEF and EAEF were verified by their very close HPLC retention times (**Figure 2**), the retention times of [^{18}F]EAEF and EAEF were 9.34 min and 8.55 min respectively. The final product was re-dissolved in saline with 0.1% ethanol and filtered through a 0.22-μm Millipore filter for further biologic evaluation.

Octanol/water partition coefficient，and Stability studies

The partition coefficient (log*P*) of [^{18}F]EAEF was determined to be 0.53 ± 0.06 (n = 3), indicating moderate hydrophilicity of the radiotracer. The stability results were showed in **Figure 3**, indicated that [^{18}F]EAEF is very stable in both saline and serum over 120 min at 37 °C.

Pharmacokinetics in mice

The pharmacokinetics of [^{18}F]EAEF in mice was also investigated using PET imaging. It was accumulated highly in liver, gallbladder and intestinal as fast as 15 min after i.v. injection, and showed faster elimination from the non-specific tissues (washout obviously at 2 h p.i. and most of the activity was excreted at 4 p.i.). The highest image contrast for tumor

detection could be obtained at 2 h p.i.. No obvious bone uptake was observed up to 4 h p.i. indicated it has good stability in mice, which consistent well with the biodistribution result.

Biodistribution study

The uptake of [^{18}F]EAEF in PR expressing tissues was efficient and selective as expected. In mice biodistribution, high radioactivity uptakes were observed in uterus (5.89 ± 0.51 % ID/g at 1 h p.i.) and ovary (4.33 ± 0.80 % ID/g at 1 h p.i.) with very good retention (5.73 ± 1.83 % ID/g and 4.05 ±0.73 % ID/g at 2 h p.i. for uterus and ovary respectively), which both of them containing PR expression after estradiol treated. For the untreated group, obviously decreased uptakes in uterus (1.58 ± 0.36 % ID/g) and ovary (1.66 ± 0.45 % ID/g) were found at 2 h p.i. when compared with the estradiol treated group, the uptake of [^{18}F]EAEF in uterus and ovary presented significant differences between estradiol treated and untreated group at 2 h($p < 0.01$). Furthermore, low background muscle uptakes (0.68 ± 0.16 % ID/g at 1 h p.i. and 0.50 ± 0.17 % ID/g at 2 h p.i.) resulted in high uterus-to-muscle ratios (8.66 and 11.46 at 1 and 2 h p.i., respectively), encouraging further evaluation. While in the nonspecific tissues, excepted spleen (3.12 ± 0.39 % ID/g at 2 h p.i.) and blood (3.46 ± 0.80 % ID/g at 2 h p.i.), all other organs like heart, liver, lung, and kidney have low radioactivity accumulation after i.v. injection. Low bone uptake was observed at 1 and 2 h p.i., indicating no defluorination of this tracer *in vivo*, which is consistent with the stability study. The notable stomach uptake may indicate that this tracer could be excreted via the intestinal system.

Imaging study

The *in vivo* microPET imaging of [^{18}F]EAEF were performed in mice to further assess its potential as a PR targeted PET tracer for PR positive breast cancer diagnosis. In MCF-7 tumor bearing mice, relative high radioactivity accumulated in tumor was observed (3.05 ± 0.07 % ID/g at 1 h p.i. and 3.15 ± 0.07 % ID/g at 2 h p.i.) with good tumor-to-muscle ratios (1.82 and 2.90 at 1 and 2 h p.i., respectively), which ensuring high contrast images could be obtained for PR positive tumor detection (**Figure 4**). Moreover, high uptakes in gallbladder, liver, and intestine at early time points after injection and decreased obviously at 2 h p.i., indicating it was metabolized through liver and intestinal system. When co-injected with precursor (compound **4**) for blocking, the uptake in MCF-7 tumor was inhibited obviously (1.84 ± 0.05 % ID/g at 2 h p.i.) with much lower tumor-to-muscle ratio (1.68). When block with non-radioactivity EAEF or pre-treated with ethisterone, the tumor uptakes and tumor-to-muscle ratios derived from PET imaging were also increased obviously (**Figure S10-13** in supporting information). In PR negative MDA-MB-231 tumor bearing mice, the tumor uptakes (1.80 ± 0.03 % ID/g at 2 h p.i.) were much lower than that of MCF-7 at all time-points after injection (**Figure 4B**). And the tumor cannot be observed due to very low image contrast. All the results showed in **Figure 4** indicating that [^{18}F]EAEF might be specifically targeting to PR which overexpressed in MCF-7 tumor.

Discussion

PR targeted radiotracer could be used to detect PR-positive breast cancer in the early stage of breast cancer. Since many steroid derivatives were labeled with ^{131}I, ^{76}Br, ^{18}F to

target breast cancer, compared with other radionuclide, the excellent physical properties of ^{18}F make it a preference among radiolabeling. In this study, we designed a novel radiotracer through click reaction between ethisterone and 2-(2-(2-azidoethoxy)ethoxy)ethyl-4-p-toluenesulfonate to get a novel radiotracer [^{18}F]EAEF as a progesterone receptor imaging agent for positron emission tomography, and the final precursor was obtained efficiently, which also has a high yield.

Although there have several radio-tracers been reported as PR targeting agent, only a few of these radiotracers, such as [^{18}F]FENP, [^{18}F]FMNP, 6α-[^{18}F]Fluoroprogesterone and [^{18}F]FPTP, have been tested in clinical trials. Among them, [^{18}F]FENP was the first progestin to be radiofluorinated(20). But it performed poorly in clinical trials due to the high adipose tissue uptake and high metabolization in humans. Same as the [^{18}F]FENP, [^{18}F]FMNP was also not satisfactory for its high lipophilicity and metabolic liability(21, 22). For 6α-[^{18}F]Fluoroprogesterone, its metabolic defluorination leads to high bone uptake(23). And for [^{18}F]FPTP, the drawbacks of low radiochemical yield (RCY), complicated and time consuming synthetic process hinder it for further application(24).

As can be seen from above, significant tracer accumulation in adipose tissue and nonspecific tissue are the common features of progesterone derivative for their relative high lipophilicity. So we synthesized our radioactive probe by introducing of short polyethyleneglycol (PEG) chain which could lower the lipophilicity obviously to reduce the nonspecific uptake. Compared with the radiotracers mentioned above, [^{18}F]EAEF displayed comprehensive advantages. For example, the bone, uterus uptake of [^{18}F]EAEF was 0.78 ± 0.16% ID/g, 5.89 ± 0.511 % ID/g % ID/g at 1 h p.i., respectively, whereas that of

6α-[^{18}F]Fluoroprogesterone was 5.726 ± 1.350 % ID/g, 0.775 ± 0.056 % ID/g at 1 h p.i., respectively(23). Consequently, the uterus-to-muscle ratio of [^{18}F]EAEF was much higher than that of 6α-[^{18}F]Fluoroprogesterone at 1 h p.i.(8.66 ± 1.32 % ID/g *vs.* 1.877 ± 0.253 % ID/g). [^{18}F]EAEF also showed a high MCF-7 tumor uptake (3.05 ± 0.07 % ID/g and 3.15 ± 0.07 % ID/g at 1 h p.i. and 2 h p.i., respectively) but low nonspecific uptake in muscle, bone, and the tumor-muscle ratio was notably higher than that in mice bearing MDA-MB-231 tumor (2.90 *vs.*1.61), showing high PR specificity. But at the same time, the radioactivity in the blood for estrogen-primed immature mice was much higher than the control group (3.46 ± 0.80 % ID/g *vs.* 1.97 ± 0.38 % ID/g) at 1 h p.i., the reason remained to be further investigated.

What's more, different from the previously reported chiral compound [^{18}F]FPTP(19), [^{18}F]EAEF is a optically pure compound and could avoid the differences in biologic properties such as metabolism or binding affinity for targets of enantiomer.

Due to the different amount of radioactivity injected and progestrone receptor existed in mice, different tumor-to-muscle ratios data and images were found in PET/CT studies. In the future, *in vivo* PR quantification with microPET imaging of more PR+ and PR- tumor-bearing mice will direct compared with that of *ex vivo* biodistribution and *in vitro* analysis. Correlation of *in vivo*, *ex vivo* and *in vitro* PR quantification results will be analyzed to validate the feasibility of quantitative PET imaging of PR with this new tracer. Whatever, [^{18}F]EAEF has suitable hydrophilicity, good *in vivo* stability, PR specificity, and high tumor-to-muscle ratio in PET imaging. All the promising properties described above indicating that [^{18}F]EAEF might be a candidate for non-invasive PET imaging of PR+ breast

cancer, but remains further investigation.

Conclusion

In summary, a novel PR targeted PET tracer [^{18}F]EAEF has been synthesized and evaluated *in vitro* and *in vivo* preliminarily. The fast and simple synthetic route with high decay-corrected RCY (30 ~ 35%) and RCP (> 98%), good stability, specific PR targeting, and high tumor uptake encourage us for further feasibility studies in the near future.

Acknowledgements

This work was supported by the National Key Basic Research Program of China (2014CB744503) and National Natural Science Foundation of China (81471707, 21271030).

References:

1. Bénard F, Turcotte E. (2005) Imaging in breast cancer: single-photon computed tomography and positron-emission tomography. Breast Cancer Res;7(4):153-62.
2. Gopalan D, Bomanji J, Costa D, Ell P. (2002) Nuclear medicine in primary breast cancer imaging. Clin Radiol;57(7):565-74.
3. Perou CM, Sørlie T, Eisen MB, van de Rijn M, Jeffrey SS, Rees CA, et al. (2000) Molecular portraits of human breast tumours. Nature;406(6797):747-52.
4. Sotiriou C, Pusztai L. (2009) Gene-expression signatures in breast cancer. N Engl J Med;360(8):790-800.
5. Carey LA, Perou CM, Livasy CA, Dressler LG, Cowan D, Conway K, et al. (2006) Race, breast cancer subtypes, and survival in the Carolina Breast Cancer Study. J Geol Soc Jam;295(21):2492-502.
6. Lerman C, Track B, Rimer BK, Boyce A, Jepson C, Engstrom PF. (1991) Psychological and behavioral implications of abnormal mammograms. Ann Intern Med;114(8):657-61.

7. Nelson HD, Pappas M, Cantor A, Griffin J, Daeges M, Humphrey L. (2016) Harms of breast cancer screening: systematic review to update the 2009 US Preventive Services Task Force recommendation. Ann Intern Med; 164, 256.

8. Tsujikawa T, Yoshida Y, Maeda H, Tsuchida T, Mori T, Kiyono Y, et al. (2012) Oestrogen-related tumour phenotype: positron emission tomography characterisation with ^{18}F-FDG and ^{18}F-FES. Brit J Radiol; 85, 1020.

9. Linden HM, Dehdashti F, editors. (2013) Novel methods and tracers for breast cancer imaging. Semin Nucl Med; 43, 324.

10. Munnink TO, Nagengast W, Brouwers A, Schröder C, Hospers G, Lub-de Hooge M, et al. (2009) Molecular imaging of breast cancer. The Breast;18:S66-S73.

11. van Kruchten M, de Vries EG, Brown M, de Vries EF, Glaudemans AW, Dierckx RA, et al. (2013) PET imaging of oestrogen receptors in patients with breast cancer. The Lancet Oncol;14(11):e465-e75.

12. Cunha S, Gano L, Morais GR, Thiemann T, Oliveira MC. (2013) Progesterone receptor targeting with radiolabelled steroids: an approach in predicting breast cancer response to therapy. J Steriod Biochem;137:223-41.

13. Weigel MT, Dowsett M. (2010) Current and emerging biomarkers in breast cancer: prognosis and prediction. Endocr Relat Cancer;17(4):R245-R62.

14. McKenna NJ, O'Malley BW. (2002) Combinatorial control of gene expression by nuclear receptors and coregulators. Cell;108(4):465-74.

15. Dowsett M, Houghton J, Iden C, Salter J, Farndon J, A'hern R, et al. (2006) Benefit from adjuvant tamoxifen therapy in primary breast cancer patients according oestrogen receptor, progesterone receptor, EGF receptor and HER2 status. Ann Oncol;17(5):818-26.

16. Van de Wiele C, De Vos F, Slegers G, Van Belle S, Dierckx RA. (2000) Radiolabeled estradiol derivatives to predict response to hormonal treatment in breast cancer: a review. Eur J Nucl Med;27(9):1421-33.

17. Deblois G, Giguère V. (2013) Oestrogen-related receptors in breast cancer: control of cellular metabolism and beyond. Nat Rev Cancer;13(1):27-36.

18. Elledge R, Fuqua S. (2000) Estrogen and progesterone receptors. Diseases of the Breast;2:471-88.

19. Reibel AT, Müller SS, Pektor S, et al. Fate of Linear and Branched Polyether-Lipids In Vivo in Comparison to Their Liposomal Formulations by ^{18}F-Radiolabeling and Positron Emission Tomography. Biomacromolecules;2015;16(3):842-51.

20. Pomper MG, Katzenellenbogen JA, Welch MJ, Brodack JW, Mathias CJ. (1988) 21-[^{18}F]fluoro-16alpha-ethyl-19-norprogesterone. Synthesis and target tissue selective uptake of a progestin receptor-based radiotracer for positron emission tomography. J Med Chem;31(7):1360-3.

21. Verhagen A, Luurtsema G, Pesser J, De Groot T, Wouda S, Oosterhuis J, et al. (1991) Preclinical evaluation of a positron emitting progestin ([^{18}F]fluoro-16α-methyl-19- norprogesterone) for imaging progesterone receptor positive tumours with positron emission tomography. Cancer Lett;59(2):125-32.

22. Dehdashti F, McGuire AH, Van Brocklin HF, Siegel BA, Andriole DP, Griffeth LK, et al. (1991) Assessment of 21-[^{18}F]Fluoro-16-ethyl-19-norprogesterone as a positron-emitting radiopharmaceutical for the detection of progestin receptors in human breast carcinomas. J Nucl Med;32(8):1532-7.

23. Choe YS, Bonasera TA, Chi DY, Welch MJ, Katzenellenbogen JA. (1995) 6α-[^{18}F] Fluoroprogesterone: Synthesis via halofluorination-oxidation, receptor binding and tissue distribution. Nucl Med Biol;22(5):635-42.

24. Lee JH, Zhou H-B, Dence CS, Carlson KE, Welch MJ, Katzenellenbogen JA. (2010) Development of [^{18}F]fluorine-substituted Tanaproget as a progesterone receptor imaging agent for positron emission tomography. Bioconjugate Chem;21(6):1096-104.

The legends of tables and figures:

Figure 1. Chemical structures of [^{18}F]FENP, [^{18}F]FMNP, 6α-[^{18}F]fluoroprogesterone and [^{18}F]FPTP.

Scheme 1. The synthetic route of tosylate precursor, EAEF and [^{18}F]EAEF. Reagents and conditions: a. TsCl, CH_2Cl_2, triethylamine, r.t. b. NaN_3, CH_3CN, 3 h, r.t. c. ethisterone, CuI, DIPEA, THF, 60 ºC, overnight. d. KF, K_{222}, CH_3CN, 90 ºC, 10 h. Radiolabeling conditions: d. K^{18}F, K_{222}, CH_3CN, 90 ºC, 20 min.

Figure 2. HPLC profile of EAEF and [^{18}F]EAEF. HPLC conditions: CH_3CN/H_2O = 40/60 (v/v), 1.0 mL/min, UV = 254 nm. t_1 = 8.55 min (retention time of EAEF) and t_2= 9.34 min (retention time of [^{18}F]EAEF).

Figure 3. *In vitro* stabilities of [^{18}F]EAEF by HPLC measurement. Incubated in mice serum and saline for 30, 60, 120 min at 37 ºC.

Table 1. Biodistribution of [^{18}F]EAEF in immature Estrogen-Primed female mice and control mice.

Figure 4. MicroPET imaging of tumor bearing mice at 15 min, 1, 2 and 4 h p.i. of [^{18}F]EAEF. PET images (tumors or tumor sites were indicated by white arrow) of MCF-7 tumor with [^{18}F]EAEF only (up), with co-injected 200 μg precursor (middle) and MDA-MB-231 tumor with [^{18}F]EAEF only (bottom) (A); Tumor uptakes (B) and Tumor-to-Muscle ratios (C) were derived from PET imaging at different time after injection of [^{18}F]EAEF.

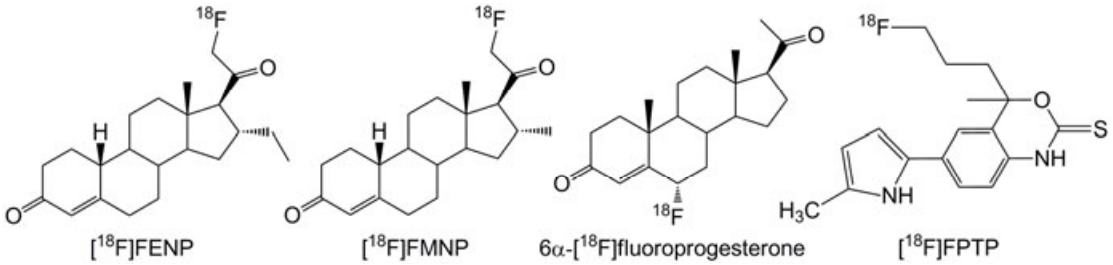

Figure 1. Chemical structures of [^{18}F]FENP, [^{18}F]FMNP, 6α-[^{18}F]fluoroprogesterone and [^{18}F]FPTP.

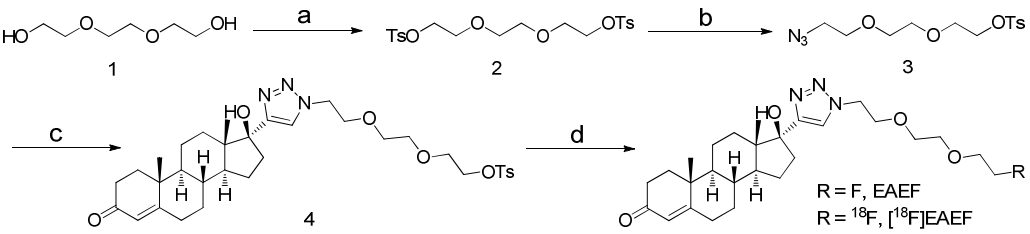

Scheme 1. The synthetic route of tosylate precursor, EAEF and [^{18}F]EAEF. Reagents and conditions: a. TsCl, CH_2Cl_2, triethylamine, r.t. b. NaN_3, CH_3CN, 3 h, r.t. c. ethisterone, CuI, DIPEA, THF, 60 ºC, overnight. d. KF, K_{222}, CH_3CN, 90 ºC, 10 h or K^{18}F, K_{222}, CH_3CN, 90 ºC, 20 min.

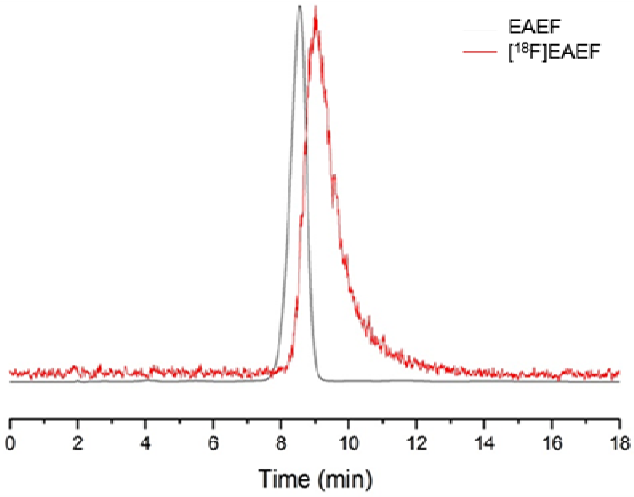

Figure 2. HPLC profiles of EAEF and [^{18}F]EAEF. HPLC conditions: CH_3CN/H_2O = 40/60 (v/v), 1.0 mL/min, UV = 254 nm. t_1 = 8.55 min (retention time of EAEF) and t_2= 9.34 min (retention time of [^{18}F]EAEF).

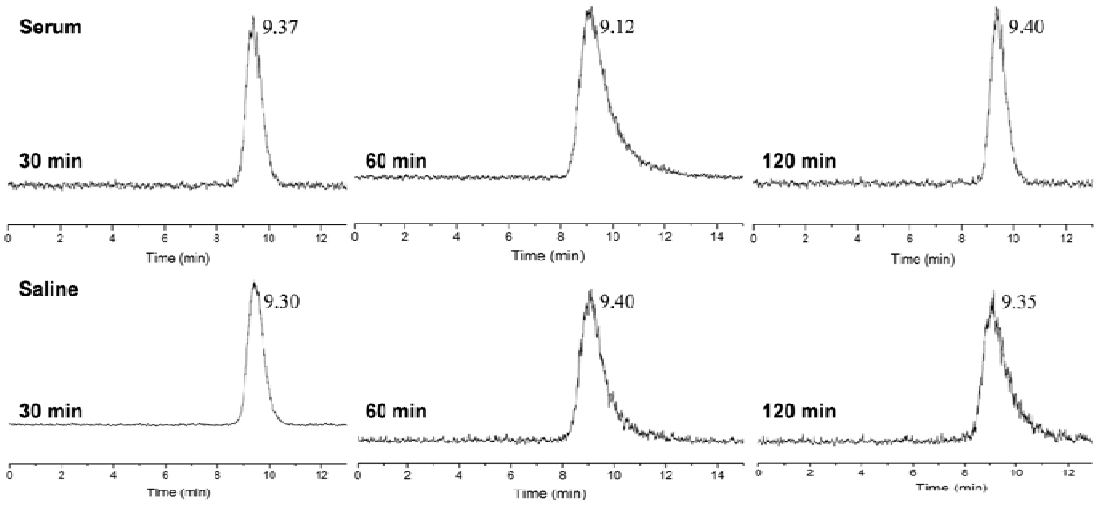

Figure 3. *In vitro* stabilities of [^{18}F]EAEF by HPLC measurement. Incubated in mice serum and saline for 30, 60, 120 min at 37 ℃.

Table 1. Biodistribution of [^{18}F]EAEF in immature Estrogen-Primed female mice and control mice.

Tissues	% ID/g ± SD[a] (n = 4)		
	1 h	2 h	2 h control
Heart	0.43 ± 0.22	0.69 ± 0.44	0.28 ± 0.07
Liver	0.30 ± 0.03	0.25 ± 0.19	0.20 ± 0.13
Spleen	3.70 ± 0.22	3.12 ± 0.39	2.25 ± 0.23
Lung	0.73 ± 0.61	0.66 ± 1.13	0.36 ± 0.12
Kidney	0.66 ± 0.66	0.47 ± 0.31	0.31 ± 0.15
Muscle	0.68 ± 0.16	0.50 ± 0.17	0.61 ± 1.52
Blood	3.01 ± 1.71	3.46 ± 0.80	1.97 ± 0.38
Bone	0.78 ± 0.16	0.65 ± 0.69	0.84 ± 0.81
Stomach	1.38 ± 0.56	0.96 ± 0.06	0.61 ± 0.17
Uterus	5.89 ± 0.51	5.73 ± 1.83	1.58 ± 0.36
Ovaries	4.33 ± 0.80	4.05 ± 0.73	1.66 ± 0.45
Uterus/Muscle	8.66 ± 1.32	11.46 ± 0.89	2.59 ± 1.21

[a] SD is standard deviation

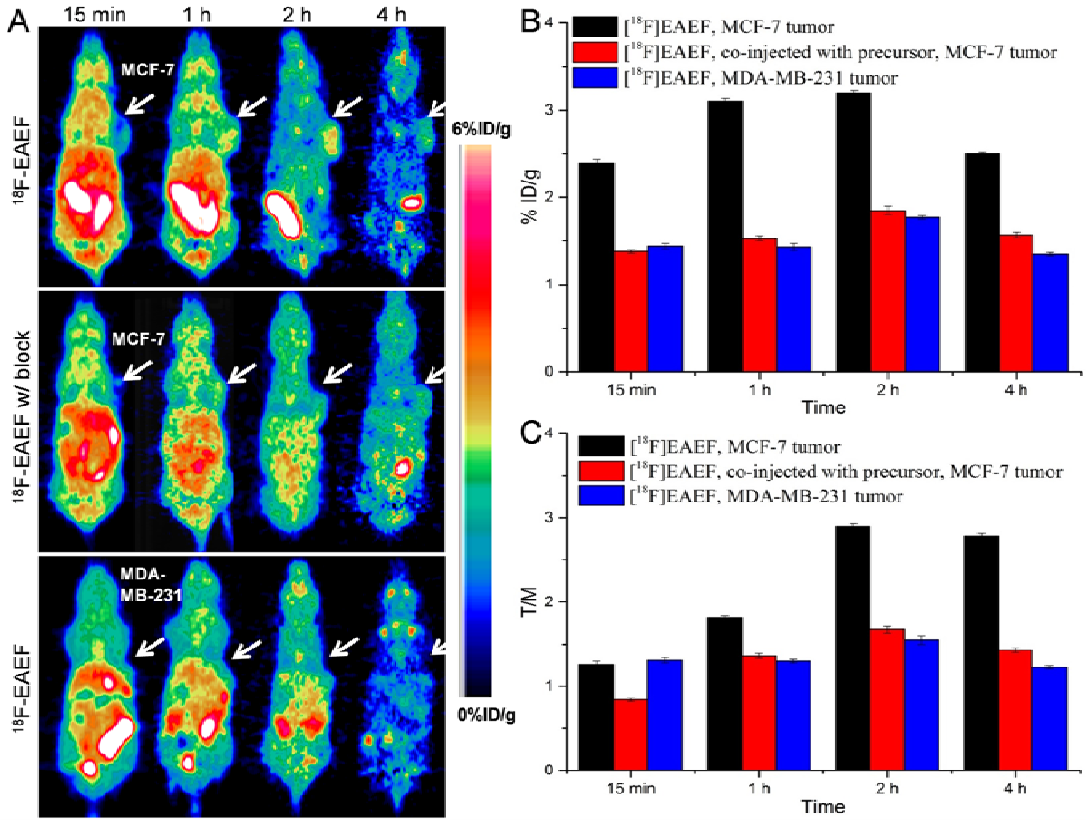

Figure 4. MicroPET imaging of tumor bearing mice at 15 min, 1, 2 and 4 h p.i. of [^{18}F]EAEF. PET images (tumors or tumor sites were indicated by white arrow) of MCF-7 tumor with [^{18}F]EAEF only (up), with co-injected 200 μg precursor (middle) and MDA-MB-231 tumor with [^{18}F]EAEF only (bottom) (A); Tumor uptakes (B) and Tumor-to-Muscle ratios (C) were derived from PET imaging at different time after injection of [^{18}F]EAEF.